



# Kharif crop characterization using combination of SAR and MSI Optical Sentinel Satellite datasets

ABHINAV VERMA<sup>1</sup>, AMIT KUMAR<sup>2</sup> and KANHAIYA LAL<sup>2,\*</sup> 

<sup>1</sup>Indian Institute of Remote Sensing, ISRO, Dehradun, India.

<sup>2</sup>Department of Geoinformatics, School of Natural Resource Management, Central University of Jharkhand, Ranchi 835 205, India.

\*Corresponding author. e-mail: [jnu.kanhaiya@gmail.com](mailto:jnu.kanhaiya@gmail.com) [kanhaiya.lal@cuja.ac.in](mailto:kanhaiya.lal@cuja.ac.in)

MS received 7 February 2019; revised 7 June 2019; accepted 15 July 2019

In the present study, the differences in the *kharif* crop reflectance at varied wavelength regions and temporal SAR backscatter (at VV and VH polarizations) during different crop stages were analyzed to classify crop types in parts of Ranchi district, East India using random forest classifier. The spectral signature of crops was generated during various growth stages using temporal Sentinel-2 MSI (optical) satellite images. The temporal backscatter profile that depends on the geometric and dielectric properties of crops were studied using Sentinel-1 SAR data. The spectral profile exhibited distinctive reflectance at the NIR (0.842  $\mu\text{m}$ ) and SWIR (1.610  $\mu\text{m}$ ) wavelength regions for paddy (*Oryza sativa*;  $\sim 0.25$  at NIR,  $\sim 0.27$  at SWIR), maize (*Zea mays*;  $\sim 0.24$  at NIR,  $\sim 0.29$  at SWIR) and finger millet (*Eleusine coracana*,  $\sim 0.26$  NIR,  $\sim 0.31$  at SWIR) during pre-sowing season (mid-June). Similar variations in crop's reflectance at their different growth stages (vegetative to harvesting) were observed at various wavelength ranges. Further, the variations in the backscatter coefficient of different crops were observed at various growth stages depending upon the differences in sowing–harvesting periods, field conditions, geometry, and water presence in the crop field, etc. The Sentinel-1 SAR based study indicated difference in the backscatter of crops (i.e.,  $\sim -18.5$  dB (VH) and  $\sim -10$  dB (VV) for paddy,  $\sim -14$  dB (VH) and  $\sim -7.5$  dB (VV) for maize,  $\sim -14.5$  dB and  $\sim -8$  dB (VV) for finger millet) during late-July (transplantation for paddy; early vegetative for maize and finger millet). These variations in the reflectance and backscatter values during various stages were used to deduce the best combination of the optical and SAR layers in order to classify each crop precisely. The GLCM texture analysis was performed on SAR for better classification of crop fields with higher accuracies. The SAR-MSI based *kharif* crop assessment (2017) indicated that the total cropped area under paddy, maize and finger millet was 24,544.55, 1468.28 and 632.48 ha, respectively. The result was validated with ground observations, which indicated an overall accuracy of 83.87% and kappa coefficient of 0.78. The high temporal, spatial spectral agility of Sentinel satellite are highly suitable for *kharif* crop monitoring. The study signifies the role of combined SAR–MSI technology for accurate mapping and monitoring of *kharif* crops.

**Keywords.** Crop monitoring; crop spectral profile; random forest classification; SAR texture; SAR–MSI image fusion.

## 1. Introduction

*Kharif* (referred as monsoon crops) is the prime crop growing season in India. The *kharif* crops, viz., *Oryza sativa* (paddy), *Zea mays* (maize), *Sorghum*

(jowar), *Pennisetum glaucum* (bajra), *Cajanus cajan* (tur), *Vigna radiata* (moong), *Vigna mungo* (urad), *Gossypium* (cotton), *Corchorus capsularis* (jute), *Eleusine coracana* (finger millet) are grown with the onset of monsoon from July to November.

Because of the presence of clouds and rain during the *kharif* season, crop monitoring using optical remote sensing data is not suitable due to its inability to see through clouds. Therefore, synthetic aperture radar (SAR), having the capability to see through cloud and light rain is being widely utilized in crop identification and monitoring (Forkuor *et al.* 2014; Du *et al.* 2015; Oyoshi *et al.* 2016). Many studies have demonstrated the potential of SAR in crop classification (Bouman and Hoekman 1993). The working capability in all weather conditions and sensitivity to crop's geometric structure and moisture content, makes SAR a viable tool in agricultural monitoring (Shao *et al.* 2001). Previous studies have exhibited the use of multi-temporal SAR data that can be very useful for classifying agricultural lands and crop growth monitoring (Chakraborty *et al.* 1997; Freeman 2007; Oyoshi *et al.* 2016). The temporal backscatter intensities can be used to differentiate different crops based on their canopy architecture and structural characteristics (Soria-Ruiz *et al.* 2009; Bargiel and Herrmann 2011). Researchers have reported the ability of SAR data for crop monitoring due to variations in backscatter characteristics during varied stages of crops (Kurosui *et al.* 1995; Aschbacher *et al.* 1995; Toan *et al.* 1997; Chakraborty *et al.* 1997; Panigrahy *et al.* 1999; Torbick *et al.* 2017). Polarimetric SAR (PolSAR) data that contains both the amplitude and phase information have also been used for crop classification in many studies (Freeman and Durden 1992; Turkar *et al.* 2012). Many researchers have also used the temporal polarimetric signature of crops for classifying the crops with higher accuracies (Skriver *et al.* 1999; Choudhury and Chakraborty 2006). Sentinel-1 SAR data is highly suitable for crop monitoring at their various growth stages due to its high spatial and temporal resolution operating at C wavelength region. Many studies have reported that the microwave energy in shorter wavelength regions (C band) are more suitable for crop studies, as they interact more with the crops due to lesser penetration compared with microwave energy at higher wavelength (S and L) band (Inoue *et al.* 2002; Brisco and McNairn 2004).

Though, remote sensing can potentially provide observations for every single field in a region for every single growing season, crop mapping and yield estimation using a single date satellite data is often inaccurate due to heterogeneity prevailed in the agricultural land (Cong *et al.* 2013; Lobell 2013). The various crops sown having varied

physical-structural properties at different phenological stage interact differently with the incoming energy, which are being utilized for accurate crop characterization (Cong *et al.* 2013; Ulaby *et al.* 1982). The temporal variation of the physiology and geometric properties over the phenological growth stages of crops from sowing to harvesting through vegetative, reproductive, and maturity; also changes their spectral and backscatter behaviour and the generated information can be exploited for crop type identification and its monitoring (Toan *et al.* 1997; Lopez-Sanchez *et al.* 2012). The spectral reflectance of crop depends upon the physio-structural characteristics of crops, whereas the SAR backscatter relies upon the crop's geometry, shape, biomass, and di-electric properties of crops. The combined use of optical and SAR datasets is therefore interesting and useful as it adds different dimensions in crop's unique identification. Many researchers have opted fusion of optical and SAR in mapping of land surface feature and resulted in increase of classification accuracy. Combining data of different systems, resolutions and wavelengths can be helpful in classifying dynamic landscapes with higher accuracies. The combination of SAR and optical data works complementary to each other and therefore yields an increased classification accuracies as optical data has rich spectral information and SAR data has more space texture information (Zhou *et al.* 2017). Forkuor *et al.* (2014) have used a combination of high-resolution multi-temporal (Rapid Eye) and dual polarimetric radar data (TerraSAR-X) to map crops of north-western Benin and shown that the integration of both the data enhanced the classification accuracy by 10–15% over the use of Rapid Eye data alone. Inglada *et al.* (2016) jointly used the multi-temporal SAR and optical data for early crop identification.

Previous studies have resulted in increased classification accuracy with inclusion of Grey level Co-occurrence Matrix (GLCM) texture parameters such as contrast, dissimilarity, homogeneity, energy, GLCM mean, GLCM variance and GLCM correlation (Johansen *et al.* 2007; Ghimire *et al.* 2010; Jia *et al.* 2012; Braun and Hochschild 2015). These different texture measures as reported in many studies had provided the classifiers with information that have helped in discriminating the land use/land cover (Franklin *et al.* 2000; Berberoglu and Curran 2004; Pearlstine *et al.* 2005). Thus, in the present study, the available temporal optical satellite data (Sentinel-2) in combination

with the SAR data (Sentinel-1) and their texture parameters were used for identification of varied crop fields in parts of Ranchi region. Since most of the crop fields (other than paddy) in Ranchi were heterogeneous, planted closed to one another, and dimensionally small, a temporal crop characterization based on both the optical and SAR data was performed to select the input layers that can best be used for crop classification. The main objective of this study was to develop the spectral profile using Sentinel-2 optical dataset and backscatter profile using Sentinel-1 SAR for three major crops present in the study area. Based on the crop spectral and backscatter profile, temporal wavelength and polarization bands with significant differences in reflectance and backscatter values were selected and used as an input layer for classification using Random Forest (RF) classifier.

## 2. Study area and data

### 2.1 Study area

The study area comprises administrative blocks of Ranchi district namely, Kanke, Mandar, and Ratu blocks, located in the eastern India (figure 1). The study area is located in the southern part of the Chotanagpur plateau, between 23°19′–23°35′N and 85°26′–84°57′E with an average elevation of 650 m and roughly covering 689.82 km<sup>2</sup> in area (Census of India 2011). The main river systems are Subarnarekha, South Koel and its tributaries. Ranchi has a hilly topography with dense tropical forest. The forest cover of the district is about 1904 km<sup>2</sup> (24.73%) (FSI 2011; <http://forest.jharkhand.gov.in>). Roughly the temperature ranges from 20° to 42°C during summer and from 0° to 25°C during winter. The total annual rainfall is about 1430 mm (56.34 inch.) out of which about 1100 mm of rainfall occurs from June to September in rainy season ([www.ranchi.nic.in](http://www.ranchi.nic.in)). The geographical area of Kanke block is 347.11 km<sup>2</sup> comprising 105 villages and total 45,390 households. Mandar has total geographical area of 238.24 km<sup>2</sup> in which total 69 villages houses 22,811 families in the block. In Ratu block, total 14,418 families are distributed over 38 villages to roughly cover 104.47 km<sup>2</sup> of the geographical area (Census of India 2011).

### 2.2 Data used

In the present study, Sentinel-1 (SAR) and Sentinel-2 (MSI) datasets and secondary data,

collected during the field survey were used. The Sentinel-2 optical data for the *kharif* crop season (June, September, October, and November of 2017) were acquired from the Sentinel Scientific Data Hub ([www.scihub.copernicus.eu](http://www.scihub.copernicus.eu)). Since, in the present study a combination of Sentinel-1 SAR and Sentinel-2 Optical data were used to map crops fields. Sentinel-1 SAR satellite data for the crop season (June–November) were also acquired from the Sentinel Scientific Data Hub ([www.scihub.copernicus.eu](http://www.scihub.copernicus.eu)). Sentinel-1 includes C-band (centre frequency 5.405 GHz) imaging operating in four exclusive imaging modes with coverage up to 400 km. It provides dual polarization capability, very short revisit times and rapid product delivery (Sentinel-1 user hand book, 2014). Data used in the study and their specification are illustrated in table 1. Field surveys were conducted in order to collect field observations of crops and to record their geolocations (figure 2b). Their geographic coordinates were recorded using a hand-held GPS, which was later used for developing crop profile and training the classifier.

## 3. Methodology

The Sentinel-1 SAR and Sentinel-2 MSI were acquired from the European Space Agency (ESA), Sentinel Scientific Data Hub (<https://scihub.copernicus.eu>) website. The satellite data were processed using the SNAP software version 5.0. Different bands in Sentinel-2 have different spatial resolution; therefore, a resampling was performed using nearest neighbour interpolation to convert the multi-size products into single-size products. Since the satellite image of 15th Oct 2017 was completely cloud free, and most of the crops were in their reproductive phase, it was used to create a land use/land cover map (LULC) of the study area, which was further used in demarcating agricultural land.

The level 1 C Sentinel datasets were corrected following orthorectification and spatial registration and later subjected to radiometric and geometric corrections. The temporal optical data were then subset to the area of interest (AOI). Random forest classifier method was adopted and the LULC was classified into six classes, *viz.*, forest, agriculture, settlement, fallow, waterbody and others. The LULC map was used to mask non-agricultural land and cloud cover from all the temporal dataset. The Sentinel-1 SAR data

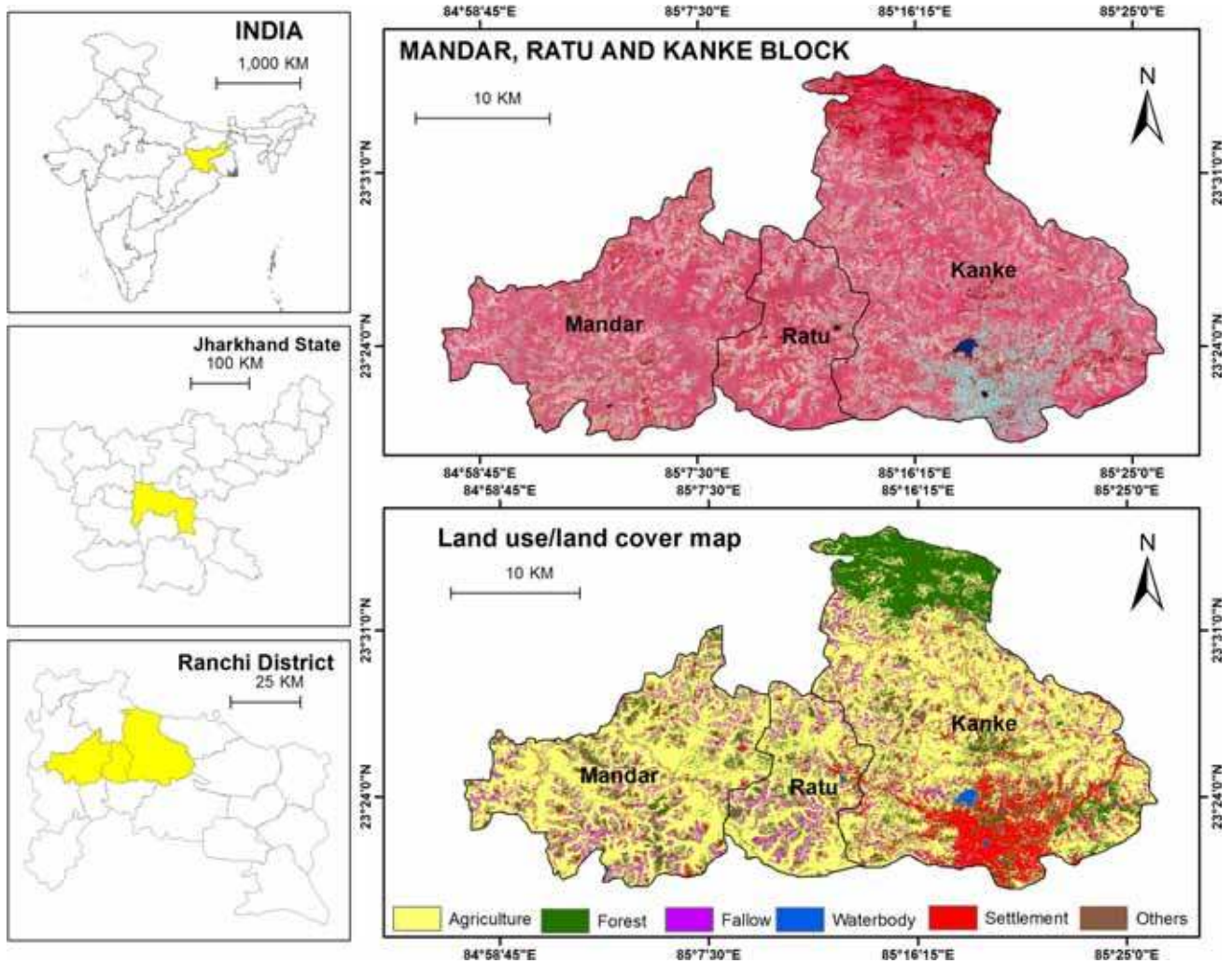


Figure 1. Study area comprising Mandar, Ratu and Kanke blocks of Ranchi district of India overlaid on Sentinel-2 satellite image (acquired on 15th Oct. 2018) and LULC map of study area.

Table 1. *Details of data used.*

Satellite data	Specification	Acquisition date
Sentinel-1	Synthetic Aperture Radar (SAR) Polarization: VV and VH Pixel spacing: 10 m Central frequency: 5.404 GHz (C band) Temporal resolution: 12 days	24.06.2017
		30.07.2017
		23.08.2017
		04.09.2017
		28.09.2017
		10.10.2017
		03.11.2017
Sentinel-2	Multi Spectral Instrument (MSI) Resolution 10 m: Blue; Green; Red; NIR Resolution 20 m: Red-Edge 1,2,3; Narrow NIR; SWIR Resolution 60 m: Coastal aerosol; water vapour; SWIR-Cirrus Temporal resolution: 5 days at equator	15.11.2017
		17.06.2017
		25.09.2017
		15.10.2017
		30.10.2017
		09.11.2017
		29.11.2017

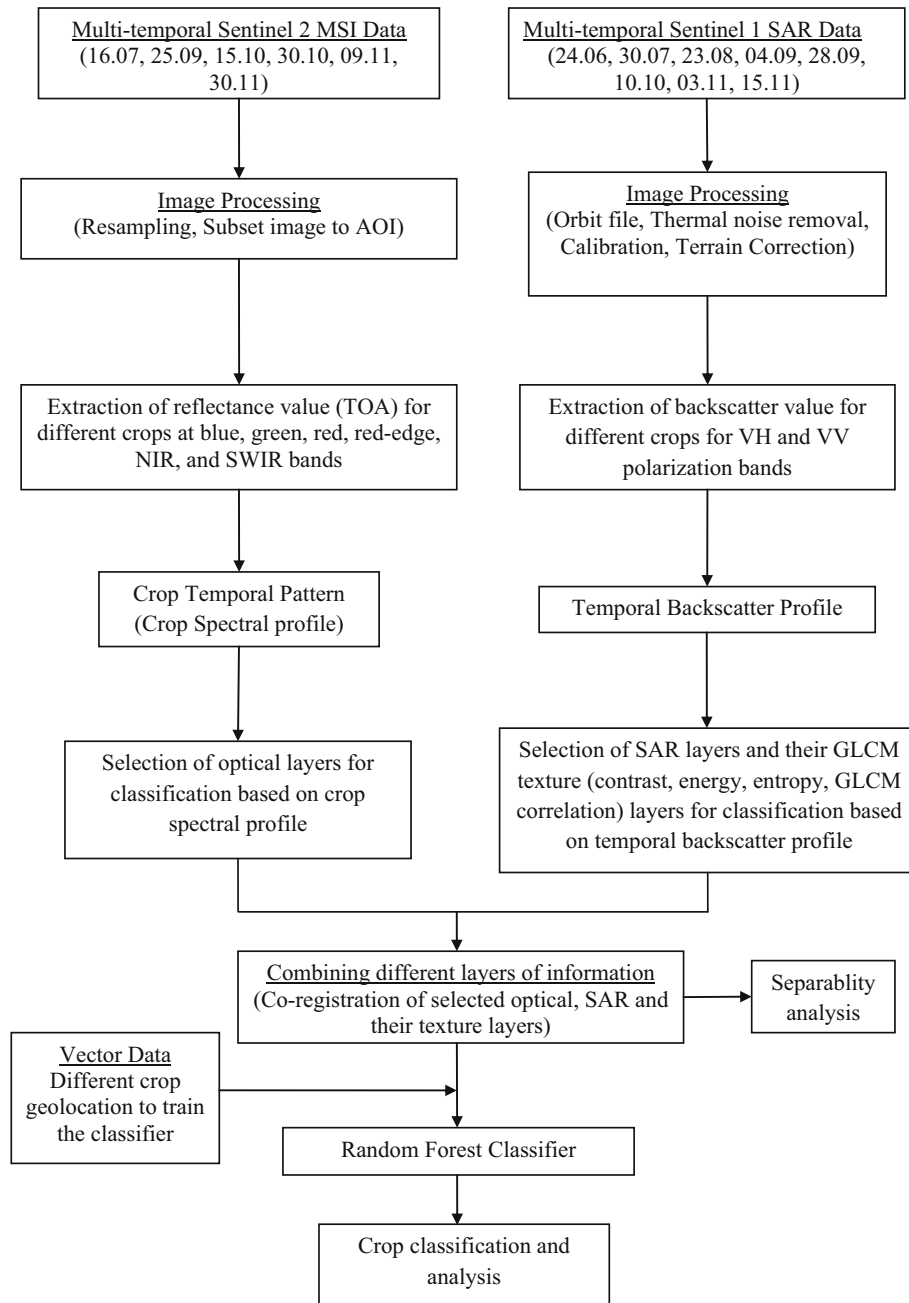


Figure 2. (a) Methodology flow chart. (b) Field map and photographs of different crop fields at various growth stages.

were processed using SNAP software. Orbit file were firstly applied to the dataset to provide accurate satellite position and velocity information, followed by thermal noise removal. The dataset was then calibrated to sigma naught. The calibrated sigma naught values were then converted into decibel using  $10 \cdot \log_{10}(\text{intensity band})$ . Finally, Range Doppler Terrain Correction (RDTC) was applied to the SAR data. The geo-location of different crops recorded during the field survey was used to generate the crop spectral and backscatter profile.

Based on the crop’s spectral and backscatter profile generated, wavelength regions and polarization bands with some differences in reflectance and backscatter values respectively, were together used as an input layer for classifying the crops using RF classifier. Additionally, GLCM texture layers, viz., energy, contrast, entropy, and correlation were also used in combination of SAR and optical data for classification. Separability analysis was performed for combined optical, SAR, and texture layers to assess its capability in discriminating the three crops present in the study area.





Crop stage	Field Photographs of various crops			Backscatter as observed in Sentinel 1
	Paddy <span style="color: yellow;">●</span>	Maize <span style="color: magenta;">●</span>	Finger millet <span style="color: red;">●</span>	
Transplanting	 85.166E 23.403 N -9.4 dB (VV) -18.5 dB (VH)	---No image---	 85.17E 23.476 N -8.2 dB (VV) -16.8 dB (VH)	
Vegetative	 85.12E 23.485 N -9.2 dB (VV) -15.8 dB (VH)	 85.176E 23.494 N -7.9 dB (VV) -14.8 dB (VH)	 85.17E 23.476 N -8.8 dB (VV) -15.4 dB (VH)	
Reproductive	 85.178E 23.422 N -10.2 dB (VV) -15.4 dB (VH)	 85.151E 23.454 N -8.4 dB (VV) -14.4 dB (VH)	 85.135E 23.48 N -8.3 dB (VV) -13.9 dB (VH)	
Mature	 85.166E 23.473 N -10.7 dB (VV) -15.4 dB (VH)	 85.304E 23.454 N -8.5 dB (VV) -15.7 dB (VH)	 85.269E 23.415 N -9.4 dB (VV) -15.2 dB (VH)	
Harvested	 85.358E 23.427 N -14.5 dB (VV) -16.2 dB (VH)	---No image---	 85.17E 23.476 N -10.2 dB (VV) -16.5 dB (VH)	

Figure 2. (Continued)

Signature for paddy, maize, and finger millet were used to compute the separability using transform divergence method. Its value greater than 1500 represents considerable separability, whereas values above 1900 show excellent separability.

#### 4. Results and discussion

##### 4.1 Crop characterization using multispectral satellite imaging

Due to the presence of cloud during most of the *kharif* cropping season, the optical Sentinel-2A satellite images of selected dates were taken into consideration under various crop growth stages, viz., pre-sown period (17th June 2017), vegetative stage (25th September 2017), reproductive stage (15th October 2017), mature stage (30th October 2017), harvesting stage (9th November 2017), and post-harvesting stages (29th November 2017). The spectral crop profiles of the crops (paddy, maize, and finger millet)

were prepared to study the variations in spectral behaviour of the various crops at different growth stages in various wavelength regions.

Most of the *kharif* crops are sown with the onset of monsoon in the month of July and are harvested in the month of November–December. June month corresponds to the pre-sown field conditions. During this period, high reflectance in the red region (0.67  $\mu\text{m}$ ) and relatively lower reflectance values at the NIR region (0.84  $\mu\text{m}$ ) than their respective values during vegetative stage (September) were observed (figure 3a, b) which also signifies the absence of crops in the fields during June and the presence of crop at vegetative stage during September. Observed increase in reflectance in NIR region (0.27 in June to 0.32 in September) and decrease in the RED region (0.16 in June to 0.12) indicate that crops at grown stage absorbs energy strongly in the visible region due to the presence of leaf pigments like carotenoids and chlorophyll and reflects very less energy back to the sensor, whereas

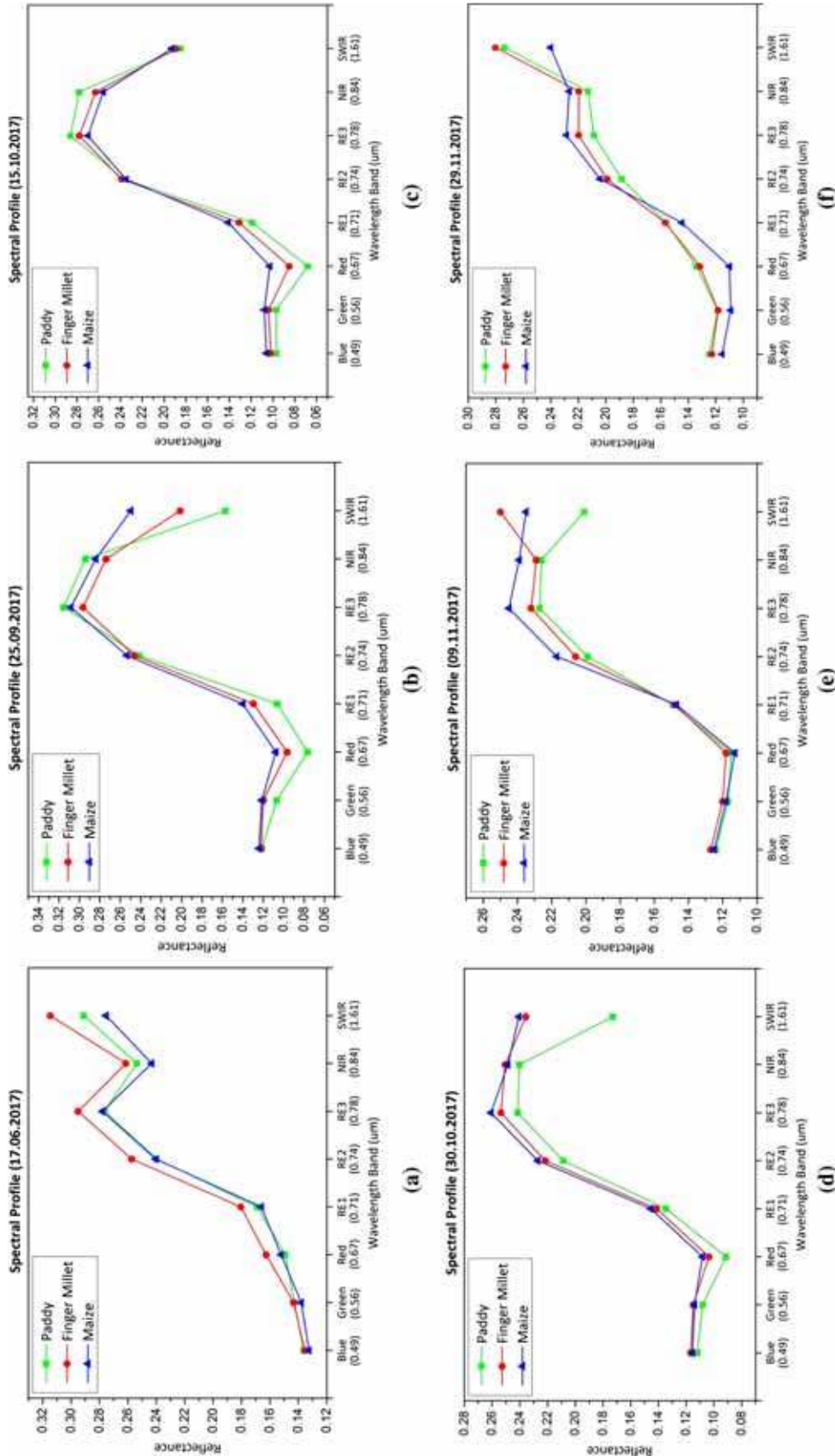


Figure 3. Crop spectral profile of paddy, finger millet and maize as on (a) 17th June, 2017 as pre-sown stage, (b) 25th September, 2017 as vegetative phase, (c) 15th October, 2017 as reproductive phase, (d) 30th October, 2017 as ripening phase, (e) 9th November, 2017 as harvesting stage, (f) 29th November, 2017 as post-harvesting stage.

in the NIR region the leaf pigment and the leaf water does not interact with radiation and therefore reflects most of the energy incident upon it. The incoming radiation in the NIR region when passes the palisade layer (presence of pigments) most of the energy is reflected without selective absorption. Therefore, when the incoming radiation interacts with green leaves, the reflectance values are lower for the visible region but it is comparatively higher in the NIR region. No significant increase in reflectance were observed between the vegetative (September) and reproductive stage (mid-October) (figure 3c). With crop maturing by early November, decline in the reflectance are observed in the NIR region (0.28 in 15th October to 0.23 in 30th October) and an increase in RED wavelength region (0.08–0.11) (figure 3d) were observed. The increase of reflectance in the RED region and decrease in NIR region is because of very sharp reduction in chlorophyll contents. Figure 3(e) illustrates decrease in reflectance values in the NIR region from 0.25 in 30th October to 0.22 in 09th November and further decreased to 0.20 for 29th November (figure 3f).

#### 4.2 Temporal backscatter profile of crops

The backscatter value is a function of the ground surface conditions, crop water content, di-electric constant, geometry, and management practices. The SAR backscatter is dynamic, it changes as the crop field condition changes from the time of sowing to harvesting (table 2). Paddy crop requires a lot of water, thus paddy fields are flooded with water in the early stages mainly at the time of sowing. Whereas, maize and finger millet crop fields do not require such flooded conditions. This

is very evident in figure 4(a and b) that represents the temporal variation at VH and VV polarization. During 30th of July significant difference in the backscatter value of paddy and other two crops was observed. Because of the specular reflection from the flooded paddy fields, low backscatter of  $\sim -18.6$  dB in VH and  $\sim -9.8$  dB in VV was observed in comparison to maize ( $\sim -13.9$  dB in VH and  $-7.6$ ) and finger millet ( $\sim -14.1$  dB in VH and  $-8.2$  dB in VV). Now as the crop grows and attains vegetative stage, increase in the backscatter values is observed because of increase in the plant height and biomass and volumetric scattering from crops canopy. The backscatter value during this stage increased from  $-18.5$  dB (VH),  $-10$  dB (VV) to  $-16$  dB (VH),  $-7$  dB (VV) for paddy as shown in figure 4(a and b). During the reproductive stage, no or very less change in the backscatter is observed due to nominal changes in crop biomass and geometry. With crop attaining mature stage, decrease in the backscatter was observed due to significant decrease in the crop's water content as the plant dries. The backscatter dropped from  $-15$  dB (VH),  $-10$  dB (VV) to  $-16.2$  dB (VH),  $-11$  dB (VV) for paddy;  $-14.5$  dB (VH),  $-8$  dB (VV) to  $-16.5$  dB (VH),  $-8.5$  dB (VV) for maize; and  $-14$  dB (VH),  $-9.5$  dB (VV) to  $-15.5$  dB (VH),  $-10.5$  dB (VV) for finger millet.

#### 4.3 Selection of input layers for classification

Data redundancy can reduce classification accuracies and computational efficiencies. Thus, proper assessment of the available datasets is necessary for selecting optimal feature space (bands) that helps in increasing the classification accuracies. The optimal layers were selected based on the spectral and backscatter profile generated at their different

Table 2. Temporal backscatter values (dB) of paddy, maize, and finger millet at VH and VV polarization.

Observation date	Paddy		Maize		Finger millet	
	VH	VV	VH	VV	VH	VV
24.06.17	-14.37	-7.01	-15.92	-8.63	-16.79	-8.87
30.07.17	-18.61	-9.72	-13.94	-7.70	-14.09	-8.10
23.08.17	-16.12	-7.20	-13.88	-7.91	-13.98	-8.59
04.09.17	-15.81	-9.20	-14.82	-7.85	-15.34	-8.74
28.09.17	-16.82	-11.48	-14.74	-7.81	-14.87	-9.13
10.10.17	-15.21	-10.15	-14.42	-8.50	-13.92	-8.34
03.11.17	-15.61	-10.62	-16.65	-9.02	-15.18	-9.47
15.11.17	-16.10	-10.89	-16.39	-8.68	-16.51	-10.25



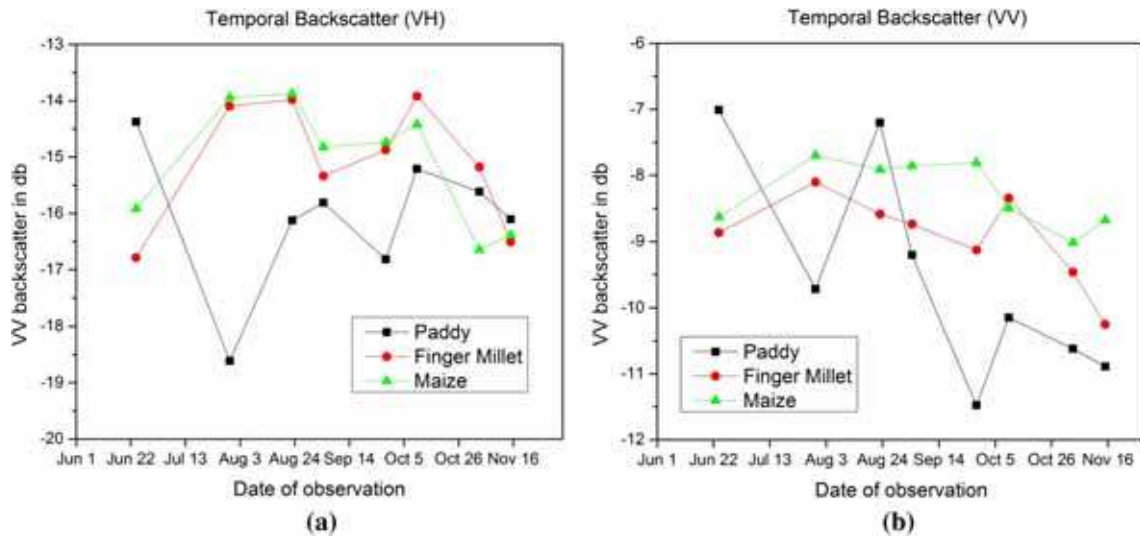


Figure 4. SAR backscatter profile for Kharif crops in (a) VH and (b) VV polarizations.

growth stages for the three major crops present in the study area.

#### 4.3.1 Selection of layers from available optical (Sentinel-2) dataset

The varied spectral response of different crops depends on their growth stages, pre-post field conditions, internal structure and geometry. Figure 3(a) represents the spectral profile for 17th June that corresponds to the pre-sown conditions of the crop fields. During this period, crops fields resulted in distinctive reflectance values at NIR region (0.25 for paddy, 0.24 for maize, 0.26 for finger millet) and SWIR wavelength regions (0.28 for paddy, 0.26 for maize, 0.31 for finger millet). The crops reflectance at their vegetative stages (25th September; figure 3b) resulted in separable values at RED (0.07 for paddy, 0.12 for maize, 0.10 for finger millet), RedEdge-1 (0.10 for paddy, 0.13 for maize, 0.12 for finger millet), and SWIR (0.15 for paddy, 0.25 for maize, 0.20 for finger millet) wavelength regions. At their reproductive stage (15th October; figure 3c), separable reflectance at RED (0.07 for paddy, 0.11 for maize, 0.08 for finger millet), RedEdge-3 (0.28 for paddy, 0.26 for maize, 0.27 for finger millet), and NIR (0.28 for paddy, 0.25 for maize, 0.26 for finger millet) wavelength regions were observed. Similar, differences in the reflectance were observed for RedEdge-3 (0.24 for paddy, 0.26 for maize, 0.25 for finger millet) band, and SWIR (0.17 for paddy, 0.24 for maize, 0.23 for finger millet) at maturing stage of crops (30th October; figure 3d). Distinguished reflectance

between crops were observed for the harvesting stage (09th November; figure 3e) at RedEdge-2 (0.19 for paddy, 0.21 for maize, 0.20 for finger millet), Red-Edge-3 (0.22 for paddy, 0.24 for maize, 0.23 for finger millet), and SWIR (0.20 for paddy, 0.23 for maize, 0.25 for finger millet) wavelength regions. Figure 3(f) represents the varied reflectance of different crops post-harvesting of the crops. They inferred distinct reflectance depending upon the crop's field condition post-harvesting. The wavelength regions with distinctive reflectance values were selected to be used as input layers for classification. The above-mentioned differences in the reflectance of different crops at different wavelength regions were exploited in order to classify the crops.

#### 4.3.2 Selection of layers from available SAR (Sentinel-1) dataset

SAR backscatter varies for different land covers in general and crops in particular depending upon their properties such as di-electric constant, biomass, and geometry. Significant differences in the crop's backscatter at VV and VH polarization were observed at different growth stages as shown in figure 4(a and b). Considerable differences in the backscatter of paddy and other two crops were observed in both VV (~-9.8 dB for paddy; ~-7.7 for maize; ~-8.3 for finger millet) and VH (~-18.5 dB for paddy; ~-13.8 for maize; ~-14.2 for finger millet) polarizations during 30th July 2017. This is due to the presence of water in paddy field and early vegetative stages of maize

Table 3. *Transformed divergence separability matrix for the three crops.*

	Paddy	Maize	Finger millet
Paddy	0	2000	1843.8
Maize	2000	0	1548.73
Finger millet	1843.8	1548.73	0

and finger millet. Similarly, distinct backscatter were observed for 4th September (Vegetative stage), where paddy was having lower biomass results in lower backscatter as compared to maize and finger millet at both VV (~-9.3 dB for paddy; ~-7.9 for maize; ~-8.7 for finger millet) and VH (~-15.9 dB for paddy; ~-14.8 for maize; ~-15.4 for finger millet) polarization. Significant differences in backscatter of the crops (~-11.5 dB for paddy; ~-7.8 for maize; ~-9.1 for finger millet) were observed during the late vegetative stage (29th September) at the VV polarization

only. Whereas the backscatter was comparable at VH polarization during this period. During late vegetative stage (10th October), varied backscatter were observed for VH polarization (~-15.3 dB for paddy; ~-14.3 for maize; ~-13.9 for finger millet), no such differences were observed in VV. During the crop's mature stage (3rd November) variations in the backscatter were observed for both VV (~-10.6 dB for paddy; ~-9 for maize; ~-9.4 for finger millet) and VH (~-15.5 dB for paddy; ~-16.5 for maize; ~-15.2 for finger millet) polarization.

#### 4.4 Crop classification using combined optical and SAR data

The SAR data for the above-mentioned periods along with their GLCM texture layers, and the wavelength bands with distinctive reflectance were combined for classifying the crops using random

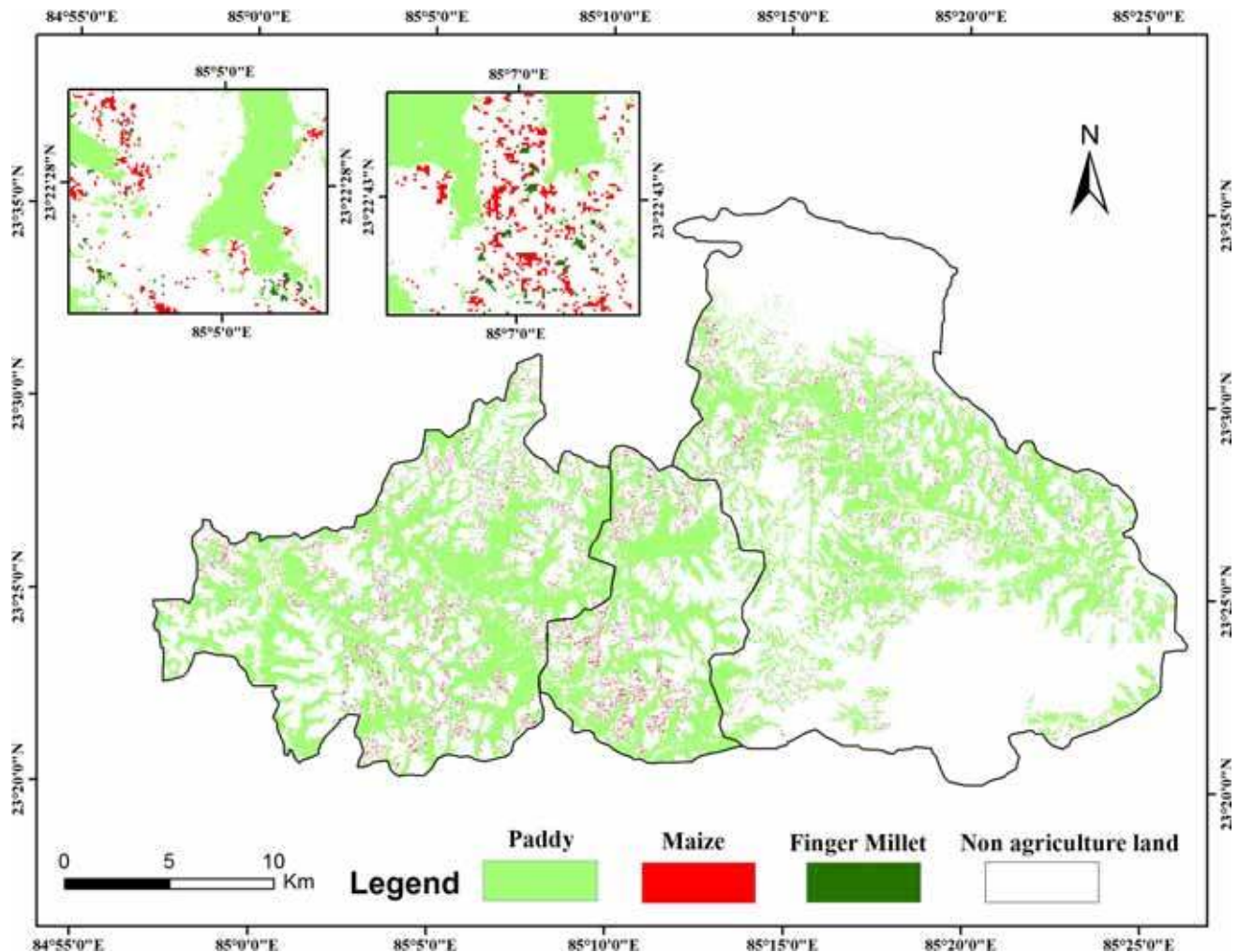


Figure 5. Map showing paddy, maize and finger millet crop area for *kharif* season 2017.

Table 4. Accuracy assessment.

Pixel	Paddy	Maize	Finger millet	Others	User accuracy (%)
Paddy	28	0	2	1	90.32
Maize	1	15	0	3	78.94
Finger millet	3	0	13	2	72.23
Others	0	1	2	22	88.00
Producer accuracy (%)	87.5	93.75	76.47	78.57	

Overall accuracy = 83.87%, Kappa coefficient = 0.78.

Table 5. Area coverage of major crops and its comparison with data of District Agricultural in parts of Ranchi district.

Crop	Area statistics (ha)	
	As reported by DAO	Based on classification of satellite data
Paddy	27,369.00	24,554.55
Maize	1841.00	1468.29
Finger millet	476.00	632.48

forest classifier. Classification based on machine learning such as random forest helps in accurate classification when a set of significant input layers are used. Further, separability analysis based on transformed divergence performed on the combined optical and SAR layers resulted in considerable separability among the three crops as shown in table 3. Excellent separability was observed between paddy and maize (2000), whereas the separability between paddy and finger millet was found to be 1843.8. A relatively low but considerable separability was observed between maize and finger millet (1548.73). The above-mentioned spectral and backscatter profile was therefore useful in selecting various wavelength and polarization bands that can be best used in classification. Many previous research studies have shown that the classification based on integration of optical, SAR and its texture components yield highly accurate classification.

The selected input layers based on the spectral and backscatter profile were used to classify the crops using RF classifier in which the geographic coordinate of crop field points recorded during the field visit were used to train the classifier. The area under paddy and other three major crops was mapped in the regions during *kharif* season 2017 (figure 5). The total 24,554.55 ha area was cropped with paddy, 1468.28 ha with

maize and 632.48 ha with finger millet during the *kharif* season 2017.

### 5. Validation and accuracy assessment

The agricultural data from the District Agriculture Office (DAO), Ranchi was collected to validate the crop maps. In the data provided by the DAO, the total crop area of different crops for *kharif* season 2017 is given (table 5). It also contains the production and yield data of major *kharif* crops. According to the data given by the DAO, the total area cropped under paddy in Kanke, Ratu, and Mandar block is 27,369 ha. The cropped area under paddy calculated on the basis of classified satellite data is 24,554.55 ha, which is almost 89.71% of the total cropped area reported by DAO. The area cropped under maize as per the classified image is 1468.29 ha and that reported by the DAO is 1841 ha. The total area under finger millet for *kharif* season 2017 is 476 ha as reported by DAO, whereas the area calculated based on the classified satellite data is 632.48 ha. Also, confusion matrix for the crop classification is represented in table 4.

### 6. Conclusion

In the present study, crop spectral profile based on Sentinel-2 MSI and backscatter profile using Sentinel-1 SAR data were used for improved classification of crops employing RF classifiers. The profiles resulted in distinctive reflectance at varied wavelength region and backscatter at VV and VH polarization for various crops at their different growth stages were useful in crop identification. Combined use of optical and SAR data add two dimensions in identification of crops as spectral reflectance is majorly governed by the physio-

structural characteristic of crops, whereas the SAR backscatter primarily depends upon the geometry, biomass, and di-electric properties of crops. The high temporal, spatial spectral agility of Sentinel satellites is highly suitable for crop monitoring.

The Sentinel-2 based *kharif* crops study indicated variations in the reflectance of different crops at various wavelength regions. Crop's reflectance at blue (0.49  $\mu\text{m}$ ) and green (0.56  $\mu\text{m}$ ) wavelength regions were not useful in crop classification as they inferred similar reflectance for the three crops. Crop's reflectance at red (0.67  $\mu\text{m}$ ) wavelength region resulted in distinctive reflectance between the three crops at vegetative, reproductive, and mature stages of crop. The reflectance curve also indicated separable reflectance for crops at NIR (0.84  $\mu\text{m}$ ) region for crop's vegetative and reproductive stages. Crop's reflectance at NIR wavelength were not separable at their mature and harvesting stages, whereas at RedEdge-2 (0.74  $\mu\text{m}$ ) and RedEdge-3 (0.78  $\mu\text{m}$ ) wavelength regions they resulted in distinctive reflectance values and were therefore useful in crop classification. SWIR (1.61  $\mu\text{m}$ ) wavelength region resulted in varied reflectance for crops during the pre- and post-crop field conditions. Further, the SAR backscatter of crops at various crop stages also resulted in distinctive values and was useful in their identification. Crop's backscatter during 30th July (transplanting stage for paddy and vegetative for maize and finger millet) resulted in significant difference between paddy and other two crops at both VV ( $\sim -9.8$  dB for paddy;  $\sim -7.7$  for maize;  $\sim -8.3$  for finger millet) and VH ( $\sim -18.5$  dB for paddy;  $\sim -13.8$  for maize;  $\sim -14.2$  for finger millet) polarization. Similarly, distinctive backscatter at VV polarization was observed during 23rd August (vegetative stage); 28th September (late-vegetative); 3rd November (mature stage). For cross-polarized VH, crops resulted in varied backscatter during 4th September (vegetative); 10th October (reproductive stage); and (3rd November) mature stage. Further, the GLCM texture parameters viz. contrast, energy, entropy and correlation of the selected SAR layers were also used in crop classification to increase classification accuracy.

The Sentinel-2A based LULC classification indicated that the 60.59% area of study area was under active agriculture and used for crop characterization. The major crops grown in the study area are paddy, maize and finger millet. The total cropped area with paddy, maize and finger millet

for *kharif* season 2017 are 24,544.55, 1468.28 and 632.48 ha, respectively. The combined use of SAR and optical data in the present study showed an overall accuracy of 83.87% and kappa coefficient of 0.78. This method of crop mapping can also be used for mapping of other crops and land features. The polarimetric SAR data with all the four polarizations and phase information can be helpful in mapping of crops with much more higher accuracies.

## Acknowledgements

The authors would like to thank editors and reviewers for their valuable comments and suggestions. Authors also convey their gratitude to the European Space Agency (ESA) for free accessibility to Sentinel-1 and Sentinel-2 satellite data. They also would like to thank District Agriculture office (DAO), Ranchi for providing with crop statistical data for *kharif* 2017.

## References

- Aschbacher J, Pongsrihadulchai A and Karnchanasutham S 1995 Assessment of ERS-1 SAR data for rice crop mapping and monitoring; *Int. Geosci. Remote Sens. Symp. IGARSS '95, Quant. Remote Sens. Sci. Appl.* **3** 2183–2185.
- Bouman B A M and Hoekman D H 1993 Multi-temporal multi-frequency radar measurements of agricultural crops during the Agriscatt-88 campaign in The Netherlands; *Int. J. Remote Sens.* **14**(8) 1595–1614.
- Berberoglu S and Curran P J 2004 Merging spectral and textural information for classifying remotely sensed images. In: *Remote Sensing Image Analysis: Including The Spatial Domain* (eds) Jong S M D and Meer F D V Remote Sens. Digital Image Process. **5** 113–136.
- Brisco B and McNairn H 2004 The application of C-band polarimetric SAR for agriculture: A review; *Can. J. Remote Sens.* **30** 525–542.
- Bargiel D and Herrmann S 2011 Multi-temporal land-cover classification of agricultural areas in two European regions with high resolution spotlight TerraSAR-X data; *Remote Sens.* **3** 859–877.
- Braun A and Hochschild V 2015 Combining SAR and optical data for environmental assessments around refugee Camps; *J. Geogr. Infor. Sci.* **1** 424–433.
- Chakraborty M, Panigrahy S and Sharma S A 1997 Discrimination of rice crop grown under different cultural practices using temporal ERS-1 synthetic aperture radar data; *ISPRS J. Photogramm. Remote Sens.* **52** 183–191.
- Choudhury I and Chakraborty M 2006 SAR signature investigation of rice crop using RADARSAT data; *Int. J. Remote Sens.* **27** 519–534.
- Census of India 2011 *District Census Hand Book, Ranchi, Jharkhand*, Government of India, Series-21, Part XII-A.

- Cong N, Wang T, Nan H, Ma Y, Wang X, Myneni R B and Piao S 2013 Changes in satellite-derived spring vegetation green-up date and its linkage to climate in China from 1982 to 2010: A multimethod analysis; *Glob. Change Biol.* **19** 881–891.
- Du P, Samat A, Waske B, Liu S C and Li Z H 2015 random forest and rotation forest for fully polarized SAR image classification using polarimetric and spatial features; *ISPRS J. Photogramm. Remote Sens.* **105** 38–53.
- Franklin S E, Hall R J, Moskal L M, Maudie A J and Lavigne M B 2000 Incorporating texture into classification of forest species composition from airborne multispectral images; *Int. J. Remote Sens.* **21** 61–79.
- Freeman A and Durden S L 1992 A three component scattering model to describe polarimetric SAR data. In: *Proceedings of the SPIE Conference on Radar Polarimetry*, CA, San Diego **1748**, pp. 213–225.
- Freeman A 2007 Fitting a two-component scattering model to polarimetric SAR data from forests; *IEEE Trans. Geosci. Remote Sens.* **45**(8) 2583–2592.
- Forkuor G, Conrad C, Thiel M, Ullmann T and Zoungrana E 2014 Integration of optical and synthetic aperture radar imagery for improving crop mapping in northwestern Benin, West Africa; *Remote Sens.* **6** 6472–6499.
- Ghimire B, Rogan J and Miller J 2010 Contextual land-cover classification: Incorporating spatial dependence in land-cover classification models using random forests and the Getis statistic; *Remote Sens. Lett.* **1** 45–54.
- Inoue Y, Kurosu T, Maeno H, Uratsuka S, Kozu T and Zielinska K D 2002 Season-long daily measurements of multifrequency (Ka, Ku, X, C, and L) and full-polarization backscatter signatures over paddy rice field and their relationship with biological variables; *Remote Sens. Environ.* **81** 194–204.
- Inglada J, Vincent A, Arias M and Marais-Sicre C 2016 Improved early crop type identification by joint use of high temporal resolution sar and optical image time series. *Remote Sens.* **8**(5) 362.
- Johansen K, Coops N C, Gergel S E and Stange Y 2007 Application of high spatial resolution satellite imagery for riparian and forest ecosystem classification; *Remote Sens. Environ.* **110** 29–44.
- Jia K, Li Q, Tian Y, Wu B, Zhang F and Meng J 2012 Crop classification using multi-configuration SAR data in the North China Plain; *Int. J. Remote Sens.* **33** 170–183.
- Kurosu T, Fujita M and Chiba K 1995 Monitoring of rice crop growth from space using the ERS-1 C-band SAR; *IEEE Trans. Geosci. Remote Sens.* **33** 1092–1096.
- Lopez-Sanchez J M, Cloude S R and Ballester-Berman J D 2012 Rice phenology monitoring by means of SAR polarimetry at X-band; *IEEE Trans. Geosci. Remote Sens.* **50** 2695–2709.
- Lobell D B 2013 The use of satellite data for crop yield gap analysis. *Field Crops Res.* **143** 56–64.
- Oyoshi K, Tomiyama N, Okumura T, Sobue S and Sato J 2016 Mapping rice-planted areas using time-series synthetic aperture radar data for the Asia-RiCE activity; *Paddy Water Environ.* **14** 463–472.
- Panigrahy S, Manjunath K R and Chakraborty M 1999 Evaluation of RADARSAT standard beam data for identification of potato and rice crops in India; *ISPRS J. Photogramm. Remote Sens.* **54** 254–262.
- Pearlstone L, Portier K M and Smith S E 2005 Textural discrimination of an invasive plant, *Schinusterebinthifolius*, from low altitude aerial digital imagery; *Photogramm. Eng. Remote Sens.* **71** 289–298.
- Skriver H, Svendsen M T and Thomsen A G 1999 Multitemporal C- and L-band polarimetric signatures of crops; *IEEE Trans. Geosci. Remote Sens.* **37** 2413–2429.
- Shao Y, Fan X, Liu H, Xiao J, Ross S, Brisco B, Brown R and Staples G 2001 Rice monitoring and production estimation using multitemporal RADARSAT; *Remote Sens. Environ.* **76**(3) 310–325.
- Soria-Ruiz J, Fernandez-Ordenez Y and McNairn H 2009 Corn monitoring and crop yield using optical and microwave remote sensing; *Geosci. Remote Sens.* **10** 405–419, <https://doi.org/10.5772/8311>.
- Toan T Le, Ribbes F, Wang L F, Nicolas F, Ding K H, Kong J A, Fujita M and Kurosu T 1997 Rice crop mapping and monitoring using ERS-1 data based on experiment and modeling results; *IEEE Trans. Geosci. Remote Sens.* **35** 41–56.
- Turkar V, Deo R, Rao Y S, Mohan S and Das A 2012 Classification accuracy of multi-frequency and multi-polarization SAR images for various land covers; *IEEE J. Sel. Top. Appl. Earth Obs. Remote Sens.* **5**(3) 936–941.
- Torbick N, Chowdhury D, Salas W and Qi J 2017 Monitoring rice agriculture across Myanmar using time series Sentinel-1 assisted by Landsat-8 and PALSAR-2; *Remote Sens.* **9**(2) 119.
- Ulaby F T, Robert Y L and Shanmugan K S 1982 Crop classification using airborne radar and Landsat data; *IEEE Trans. Geosci. Remote Sens.* **1** 42–51.
- Zhou T, Pan J and Zhang P 2017 Mapping winter wheat with multi-temporal SAR and optical images in an urban agricultural region; *Sensors (Switzerland)* **17** 1–16.